Multi-Modal Change Detection, Application to the Detection of Flooded Areas: Outcome of the 2009–2010 Data Fusion Contest

Nathan Longbotham, *Student Member, IEEE*, Fabio Pacifici, *Member, IEEE*, Taylor Glenn, *Student Member, IEEE*, Alina Zare, *Member, IEEE*, Michele Volpi, *Student Member, IEEE*, Devis Tuia, *Member, IEEE*, Emmanuel Christophe, *Member, IEEE*, Julien Michel, *Associate Member, IEEE*, Jordi Inglada, *Member, IEEE*, Jocelyn Chanussot, *Fellow, IEEE*, and Qian Du, *Senior Member, IEEE*

***Abstract*—The 2009–2010 Data Fusion Contest organized by the Data Fusion Technical Committee of the IEEE Geoscience and Remote Sensing Society was focused on the detection of flooded areas using multi-temporal and multi-modal images. Both high spatial resolution optical and synthetic aperture radar data were provided. The goal was not only to identify the best algorithms (in terms of accuracy), but also to investigate the further improvement derived from decision fusion.**

This paper presents the four awarded algorithms and the conclusions of the contest, investigating both supervised and unsupervised methods and the use of multi-modal data for flood detection. Interestingly, a simple unsupervised change detection method provided similar accuracy as supervised approaches, and a digital elevation model-based predictive method yielded a comparable projected change detection map without using post-event data.

***Index Terms*—Change detection, data fusion, decision fusion, flood detection, high spatial resolution, optical, synthetic aperture radar.**

Manuscript received September 12, 2011; revised October 24, 2011; accepted November 28, 2011. Date of publication January 31, 2012; date of current version February 29, 2012. This work was supported in part by the Swiss National Science Foundation under Grant 200021-126505 and Grant PZ00P2-136827.

N. Longbotham is with the Aerospace Engineering Sciences Department, University of Colorado, Boulder, CO 80302 USA.

F. Pacifici is with DigitalGlobe Inc., Longmont, CO 80504 USA.

T. Glenn is with the Department of Computer and Information Science and Engineering, University of Florida, Gainesville, FL 32601 USA (e-mail: tcg@cise.ufl.edu).

A. Zare is with Department of Electrical and Computer Engineering, University of Missouri, Columbia, MO 65211 USA (e-mail: zarea@missouri.edu).

M. Volpi is with Institute of Geomatics and Analysis of Risk, University of Lausanne, 1015 Lausanne, Switzerland (e-mail: michele.volpi@unil.ch).

D. Tuia is with the LASIG Laboratory, EPFL, 1015 Lausanne, Switzerland (e-mail: devis.tuia@epfl.ch).

E. Christophe was with the Centre for Remote Imaging, Sensing and Processing (CRISP), National University of Singapore, Singapore 119260, and is now with Google Inc., Mountain View, CA 94043 USA (e-mail: emmanuel.christophe@gmail.com).

J. Michel was with Communications et Systèmes, 31506 Toulouse, France, and is now with the Centre National d'Études Spatiales, Toulouse Cedex 09, 34401 France (e-mail: julien.michel@cnes.fr).

J. Inglada is with the Centre National d'Études Spatiales, Toulouse Cedex 09, 34401 France (e-mail: jordi.inglada@cesbio.cnes.fr).

J. Chanussot is with GIPSA-Lab, Grenoble Institute of Technology, Grenoble, 38402 France (corresponding author, e-mail: jocelyn.chanussot@gipsa-lab.grenoble-inp.fr).

Q. Du is with the Department of Electrical and Computer Engineering, Mississippi State University, Mississippi State, MS 39762 USA (e-mail: du@ece.msstate.edu).

Color versions of one or more of the figures in this paper are available online at http://ieeexplore.ieee.org.

Digital Object Identifier 10.1109/JSTARS.2011.2179638

I. Introduction

THE Data Fusion Technical Committee (DFTC) of the IEEE Geoscience and Remote Sensing Society serves as a global, multi-disciplinary network for geospatial data fusion, connecting people and resources. It aims at educating students and professionals, and promoting the best practices in data fusion applications [1]. The Data Fusion Contest has been annually organized by the DFTC since 2006 [2]–[4]. It is open not only to IEEE members, but to everyone, with the aim of evaluating existing methodologies at the research or operational level to solve remote sensing problems using data from different sources.

In 2009–2010, the aim of the Contest was to perform change detection using multi-temporal and multi-modal data. Two pairs of data sets were available over Gloucester, UK, before and after a flood event occurred in November 2000. The class "change" was the river and class "no change" was the areas that stayed dry. The optical and synthetic aperture radar (SAR) images were provided by the Centre National d'Études Spatiales (CNES). The participants were allowed to use a supervised or an unsupervised method with all the data, the optical data only, or the SAR data only. Accordingly, six categories were considered to account for different submissions:

Supervised—All data
Supervised—Optical data
Supervised—SAR data
Unsupervised—All data
Unsupervised—Optical data
Unsupervised—SAR data

As for the previous editions of the Contest, the ground truth used to assess the results was not provided to the participants. However, about 60,000 samples were made available for training the supervised methods.

The single results among all categories were validated and ranked using the estimated Cohen's Kappa statistic (or K coefficient). Then, the best 5 individual algorithms among all submissions were used to perform decision fusion with majority voting.

The four winning algorithms are briefly described as follows:

1) Supervised method with all data: a supervised neural network approach was proposed to exploit both the optical and SAR images to create a change detection map; the

flooded and non-flooded map regions were successively homogenized using a minimum mapping unit morphological operator.
2) Supervised method with optical data only: it used spatial contextual features extracted from the near-infrared (NIR) band of the post-event image (where the flooded areas were more distinguishable); the morphological features extracted were stacked to form a ten-dimensional multi-temporal data set and fed as inputs to a support vector machine (SVM) classifier.
3) Unsupervised method with optical data only: this technique also exploited the relatively high absorption of water in the NIR band to guide an unsupervised clustering algorithm.
4) A predictive model: a predictive model was used to project post-flood change by exploiting a digital elevation model (DEM). This model may be helpful to rescue planning during the very first hours after a flood occurs when the post-event data may still be unavailable.

This paper is organized as follows. First, a short literature review is illustrated in Section II, whereas the data set used for the Contest is described in Section III. The four winning algorithms are presented in Sections IVto VII. Finally, decision fusion is discussed in Section VIII, as well as conclusions and perspectives drawn by this Contest.

II. Related Work

In the past few years, there has been a growing interest in the development of change detection techniques for the analysis of multi-temporal imagery. This interest stems from the wide range of applications in which change detection methods can be used, such as urban and environmental monitoring, agricultural and forest surveys, and, as with this year's Contest, disaster management. Supervised and unsupervised approaches proposed in the literature are here briefly reviewed.

A. Supervised Change Detection

Supervised change detection aims at defining classification rules by modeling labeled examples provided by the user, accounting for the different classes of land-cover transitions. When dealing with high to very high spatial resolution (VHR) imagery (either optical or SAR data sets), the comprehensive labeled set can be extracted by photo-interpretation of the multi-temporal images.

Two main supervised approaches are found in the literature: post classification comparisons [5], where classification is performed independently at each time instant, and a successive comparison defines a change map; and multi-date classification [6], where multi-temporal information is considered simultaneously for classification.

In the first case, a logical comparison is most often performed on the classification outcomes at each time instant [7]. This approach may not be optimal for VHR imagery, because it may accumulate single image classification errors. As a result, post-classification comparison generally provides noisy maps, and changes in viewing acquisition can make the final map difficult to be interpreted. To avoid these errors, an approach based on post-classification masking has been proposed in [8], where a binary neural network is used to remove spurious detections, or in [9], where change vector analysis [10], [11] is used for the same purpose.

On the contrary, multi-date classification converts change detection into a multi-temporal classification problem. The two images are combined into a multi-temporal representation (through vector stacking or multi-variate difference) before analysis and a model is defined using this multi-temporal feature space. For example, supervised multi-temporal classification was implemented using SVM in [12], while in [13] Camps-Valls *et al.* defined a set of specific kernel functions for the problem of multi-temporal classification. Finally, recent works studied the relationship between the efficiency of change detectors and scarceness of labeled information using semi-supervised methods [14], [15].

B. Unsupervised Change Detection

Much of the recent work on unsupervised multi- and hyperspectral image analysis has attempted to integrate spatial information to improve algorithm performance [16]. In [17], a fuzzy clustering approach that incorporates spatial information for segmentation of remote sensing data sets was investigated. A hierarchical clustering algorithm that exploits spatial information for segmentation was described in [18]. In [19], spatial-spectral clustering using Gaussian Markov random fields for scene segmentation and anomaly detection was presented. Similarly, integration of spatial information into spectral unmixing of multi- and hyper-spectral data was investigated in [20]–[22].

The integration of domain specific knowledge has been used in a number of systems for detection of various materials or objects. This knowledge may be based on the sensing platform, subjects being sensed, or physical phenomena affecting the system. Such techniques are discussed in [23] where the expected spectral shape of vegetation in the long wave infrared was used to guide an unsupervised algorithm for the detection of vegetation in remotely sensed data. In [24], bridges are detected using rules which leveraged the known spatial arrangements of bridge pixels with respect to water and concrete in conjunction with classification algorithms.

In the context of SAR image analysis, the problem of unsupervised change detection has been addressed with less emphasis with respect to optical imagery. Recent studies have investigated different aspects, including image de-speckling and optimal threshold selection [25], [26], whereas statistical and fuzzy approaches have been discussed in [27].

III. Data Sets

The data used in the Contest included two observations, one before and one after the flood event, from two separate satellite instruments: the optical Système Probatoire d'Observation de la Terre (SPOT) and the SAR instrument aboard the European Remote Sensing 1 (ERS-1).

The SPOT satellite, operated by the Spot Image company, is a four band optical platform. Three of the channels cover the spectral range 0.50 μm to 0.89 μm and the fourth is a panchromatic band with a spectral range from 0.50 μm to 0.73 μm. The

TABLE I
SPECTRAL BANDS OF THE OPTICAL SPOT SATELLITE. ONLY THE MULTI-SPECTRAL BANDS WERE USED AS INPUT FOR THE CHANGE DETECTION PROBLEM

Band Name	Wavelength Range	Spatial Resolution
XS1	0.50 - 0.59 μm (green)	20 m x 20 m
XS2	0.61 - 0.68 μm (red)	20 m x 20 m
XS3	0.78 - 0.89 μm (near IR)	20 m x 20 m
PAN	0.50 - 0.73 μm	10 m x 10 m

TABLE II
ERS SAR SATELLITE SPECIFICATIONS

Band Name	C-band
Frequency	5.3 GHz
Polarization	Linear VV
Wave Mode	
Spatial Resolution	10 m
Swath Width	5 km
Image Mode	
Spatial Resolution	30 m
Swath Width	100 km

spatial resolution is nominally 20 m at nadir for the multi-spectral bands and 10 m at nadir for the panchromatic. The satellite is in a sun-synchronous polar orbit and has a steerable strip-selection mirror that can collect imagery up to 27° off-nadir. This pointing capability gives the satellite a revisit rate of 4–5 days. A summary of the SPOT specifications is provided in Table I.

The ERS SAR satellite, launched by the European Space Agency, is a C-band platform. The satellite is in a sun-synchronous polar orbit with a revisit time of 35 days. The SAR instrument can operate in two modes: image and wave. The wave mode provides a spatial resolution of 10 m with a swath width of 5 km. The image mode provides a larger area observation with a swath width of 100 km but reduces the spatial resolution to 30 m. The imagery used in this Contest was collected in wave mode. Its specifications are summarized in Table II.

The SPOT images distributed during the Contest contained only the multi-spectral bands (i.e., no panchromatic information was available to the participants). These images were acquired on September 1999 and November 2000, while the ERS-1 images were acquired on October 1999 and November 2000. The before- and after-flood images from both platforms are shown in Fig. 1, whereas the ground survey used to validate the change detection results uploaded by the participants is shown in Fig. 2.

IV. SUPERVISED CHANGE DETECTION—ALL DATA

The methodology discussed in this section was very similar to the winning approaches in previous years' Contests. The methods from 2007 [3] and 2008 [4] share the same neural network topology as the one discussed here. However, the input and output of the network were different as required by the data and change detection problem, but the internal architecture was similar. Also, both the learning and pruning methods were identical.

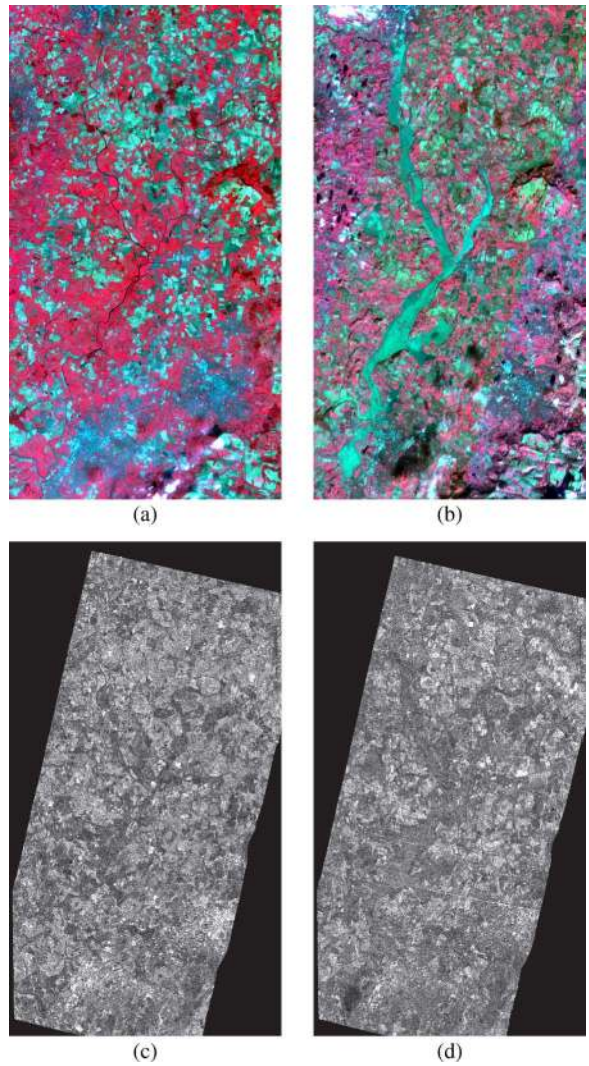

Fig. 1. Three band optical and single amplitude SAR data, collected before (left) and after (right) the flood event, provided as input to the change detection problem from the SPOT (a) and (b), and ERS (c) and (d) satellites.

Fig. .2. Ground survey used for the Contest.

Neural networks are nonlinear statistical models capable of modeling complex systems [28]. They are composed of a set of

interconnected nodes, called neurons, each connected by a network of weighted inputs. Each neuron receives input from either external sources or neighboring nodes. It then uses an internal mechanism (network and activation functions) to compute an output value from the weighted inputs that is then propagated on to the nodes it is connected to [29]. The nodes, in turn, calculate an output value from their weighted inputs and internal mechanisms. After this process is complete throughout the network, the weightings at each neuron are optimized by minimizing an error function measuring the learned accuracy of the network against known input/output values.

This arrangement provides neural networks the capability to model highly nonlinear systems in situations where the statistical distribution of the data is poorly understood [30]. This is often the case in change detection where a large range of data from multiple sensing platforms, as well as data derived from these sources, can be available.

Neural networks have been used for land-cover change detection for decades. Early attempts focused on the capability of basic neural networks to accurately predict change in multiple remote sensing applications [31]–[33]. More recent studies have focused on alternative network types [34], [35] and on neural networks as part of change detection systems [36].

Since neural networks operate on the principle of weighted inputs, it is advantageous to normalize the input data space. This should result in a faster training process as well as increases accuracy for the resulting network [37]. In the presented method, the data was normalized in the range $[-1, +1]$.

As discussed above, the input data consisted of a before and after image from both a three-band optical and single-band SAR satellite. From this information, and the desired change cases, the input and output nodes of the network were fixed: eight input nodes corresponding to the eight bands of before and after observation data, and two output nodes corresponding to the two classification cases of interests (flooded and non-flooded).

The design of the hidden layer is the subject of a large discussion in current literature; however, it is generally acknowledged that no more than two layers are needed and that layer depth can be pruned to optimize the network complexity [38]. For this Contest, computational power was not a constraint. Therefore, the network was designed at the more complex end of literature recommendations and pruned to an optimized topology. The internal structure, before pruning, consisted of two internal layers of 40 nodes each. The network was trained with the scaled conjugate gradient method and used magnitude-based pruning to optimize the topology [38].

The pixel-level classification produces maps that directly reflect the spectral-spatial variability of the image, producing a sort of "salt and pepper" noise driven by valid spectral information. This can be a limitation to classification accuracy when compared against ground survey regions that are often considered uniform by human experts. In the current study, this can be seen in small patches of earth exposed in the middle of a flooded field or regions of standing water in an otherwise non-flooded area.

This effect was addressed through the use of morphological post processing [39] to implement a minimum mapping unit and homogenize stranded pixels in the flooded and non-flooded regions. The implementation used a sieve and clump process to filter out groups of pixels below a specified size. Clusters of pixels below a given filter size were removed using a blob process. The removed pixels were then refilled using morphological dilation from the surrounding classes [40].

TABLE III
CONFUSION MATRIX AND K COEFFICIENT FOR THE SUPERVISED CHANGE DETECTION—ALL DATA

		Prediction		
	$K = 0.703$	Change	No Change	%
True	Change	643,079	220,905	**74.4**
	No Change	255,463	8,670,953	**97.1**
	%	**71.6**	**97.5**	

In the case of change detection, removing regions of a given class below a certain pixel number threshold and filling the area with the other class was a relatively simple process. For the Contest, the filter size chosen was 51 pixels. This provided well segmented change regions without over simplifying the spatial structure of the flooded region. This step generated the final classification map submitted for the competition, which produced a K coefficient of 0.703. The confusion matrix in Table III further details the distribution of accurately predicted change detection pixels.

V. SUPERVISED CHANGE DETECTION—OPTICAL DATA

The methodology discussed in this section considers the use of cascade contextual features in conjunction with support vector machines. Contrarily to the model presented in the previous section, spatial regularization is intrinsic to the model, since it is introduced by the use of contextual information in the input information. The use of contextual information is not fully exploited in the supervised change detection literature, although the benefits of including such as variables are clearly demonstrated for classification tasks [41]–[43]. In [44], the advantages of deploying reconstruction morphological operators in the change vector analysis framework have been demonstrated. In [45] a contextual parcel-based multi-scale approach to unsupervised change detection is presented. Finally, in [46] textural and morphological filters are studied extensively and their importance for successful VHR supervised change detection is analyzed.

Mathematical morphology [40] is a collection of contextual filters based on set theory. They extract local characteristics of gray-level images, and, at different scales, provide information about shape and structure of the objects in the scene [47], [48]. Morphological reconstruction filters are considered in this study to maintain the spatial information necessary to detect the flooding limits precisely. These filters—opening and closing by reconstruction—preserve objects' shapes, while returning respectively local minima or maxima, and smoothing the high local variances that affect VHR images.

Four features have been used. The first two have been extracted using opening by reconstruction on the NIR band at time instant t_2, where the flooded area was the most visible. Two sizes of the structuring elements (the moving windows detecting local valleys/peaks) have been considered to account for

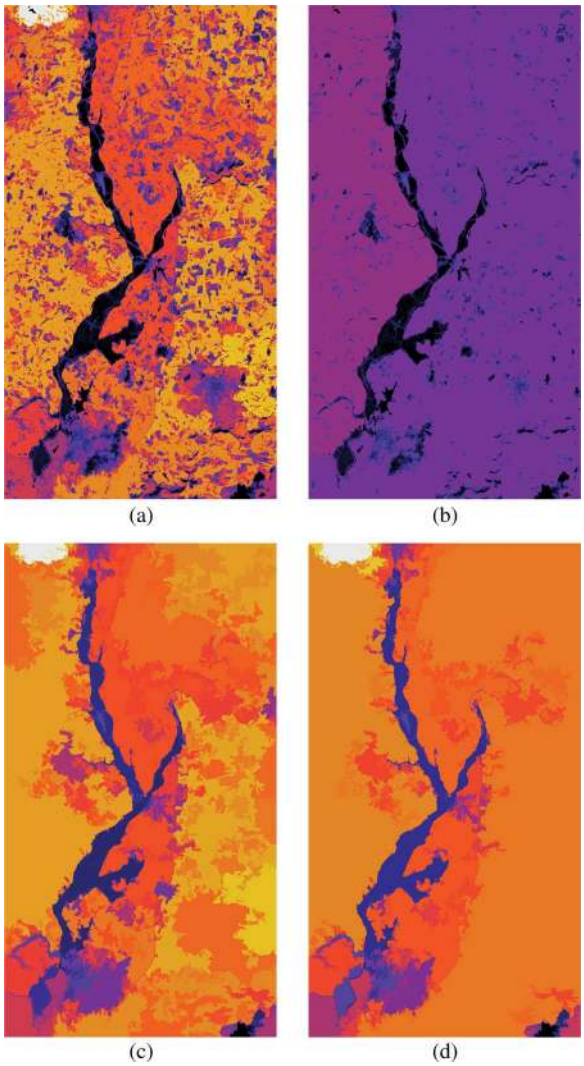

Fig. 3. Contextual features extracted from the near infrared band at time t_2. (a) Opening by reconstruction with circular structuring element of radius 40 pixels. (b) Opening by reconstruction with circular structuring element of radius 100 pixels. (c) Closing by reconstruction with circular structuring element of radius 60 pixels using erosion of panel (a) as starting marker. (d) Closing by reconstruction with circular structuring element of radius 90 pixels using erosion of panel (a) as starting marker.

different scales of smoothing: circular elements of 40 and 100 pixels in radius. The choice of wide elements resulted from the large extent of the flooded area. Results of this filtering, $\mathbf{x}^{or}$, are reported in Figs. 3(a) and 3(b), respectively. In both cases, light areas saturate, clearly defining the shape of the flooded area.

However, the opening by reconstruction operators do not filter out small and medium sized crops areas showing low NIR values (resulting in dark objects). In order to eliminate these undesired low-valued patches, we applied closing by reconstruction (i.e. the inverse process) to the opening by reconstruction feature of Fig. 3(a): by doing so, the opening image is dilated and the small patches are absorbed by the high-valued neighboring patches. Thanks to the shape-preserving character of the reconstruction filter, the central flooded area remains geometrically unchanged, although the average value of its segments increases (to the maximal value encountered in the flooded area reconstructed in Fig. 3(a)). The results of this morphological cascade filter $\mathbf{x}^{cr}$ are reported in Figs. 3(d) and 3(e) for circular structuring elements of radius 60 and 90 pixels respectively.

Successively, the original multi-temporal bands and the extracted contextual features were stacked in a 10-dimensional vector

$$\mathbf{x} = [\mathbf{x}_{\mathrm{G}}^{t_1}, \mathbf{x}_{\mathrm{R}}^{t_1}, \mathbf{x}_{\mathrm{NIR}}^{t_1}, \mathbf{x}_{\mathrm{G}}^{t_2}, \mathbf{x}_{\mathrm{R}}^{t_2}, \mathbf{x}_{\mathrm{NIR}}^{t_2}, \mathbf{x}_{40}^{or}, \mathbf{x}_{100}^{or}, \mathbf{x}_{60}^{cr}, \mathbf{x}_{90}^{cr}].$$

Each feature has been converted to standard scores prior to stacking.

From the ground truth provided, 4000 pixels (2000 for changes related to water and 2000 corresponding to unflooded areas) have been extracted for the training phase. The associated multi-temporal pixel was then used to train a one-against-all SVM implemented using the Torch 3 library [49]. A radial basis function kernel has been used. Model selection has been performed by grid search to find SVM optimal parameters σ and C.

The final submission produced a K coefficient of 0.650. The confusion matrix in Table IV further details the distribution of accurately predicted change detection pixels.

TABLE IV
CONFUSION MATRIX AND K COEFFICIENT FOR THE SUPERVISED CHANGE DETECTION—OPTICAL DATA

		Prediction		
	$K = 0.650$	Change	No Change	%
True	Change	529,300	334,684	**61.2**
	No Change	168,637	8,757,779	**98.1**
	%	**75.8**	**96.3**	

VI. UNSUPERVISED CHANGE DETECTION—OPTICAL DATA

Clustering techniques have been widely used in the multi-spectral and hyper-spectral literature [50]. For example, in [51], a fuzzy clustering approach was used to identify land-cover types in Landsat, QuickBird, and MODIS data. The approach described in this section used clustering techniques to fuse the information from the three spectral bands and produce labels for each pixel by content grouping. Successively, contextual information was used to produce consistent labels over larger areas. Finally, physics-based rules were used to select labeled groups containing flood water.

The first step was to pre-process the data to remove some anomalies. Pixel values for each channel were integers in the range [0, 127]. A few anomalous pixels were found with a -128 value across bands, and such pixels were simply clipped into standard bounds by setting their value to 0.

The optical data was then clustered into ten groups using the fuzzy C-mean clustering algorithm with a Euclidean distance measure. Clustering was performed using only the three optical band values for each pixel (i.e., no spatial information was used). Pixels were then assigned the label of the cluster to which they had highest membership. The clustering was performed using all of the approximately 9.8 million pixels in the image, and generated robust results to a qualitative visual inspection.

Upon close inspection of the clustering result in Fig. 4, it is possible to note that the large central flooded/river section was assigned to cluster 5 (cyan). Many areas of land corresponding

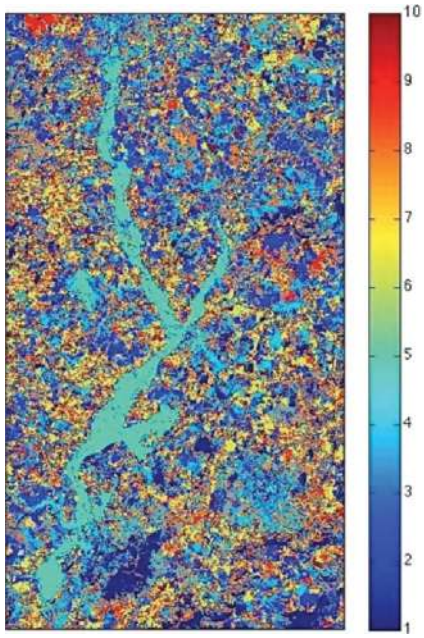

Fig. 4. Pixels assigned to color/class by highest Fuzzy C-Means cluster membership.

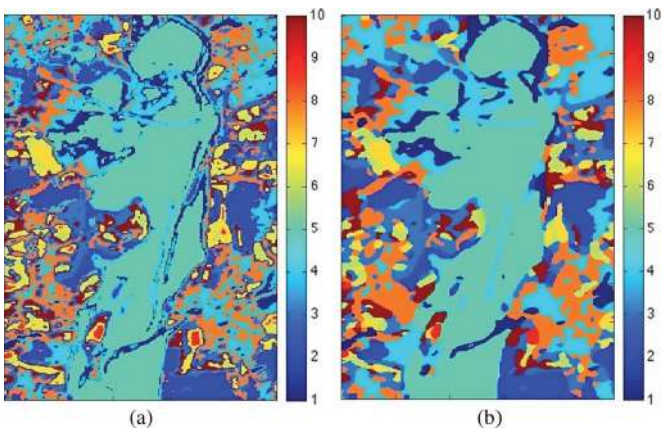

Fig. 5. (a) Non-smoothed cluster labels (detail view of Fig. 4). (b) Cluster labels after smoothing by voting in 5 × 5 window.

to agricultural fields were assigned to clusters 6 and 7 (yellow and light orange), whereas areas in shadow from cloud cover were assigned to cluster 1 (dark blue).

The next step integrated spatial information to the cluster labels by applying a neighborhood-voting procedure. This step was performed to remove any small, discontinuous, or noisy clusters. Cluster labels for each pixel were smoothed using voting. The voting method reassigned each pixel the value of the most frequently occurring label within a 5 × 5 pixel neighborhood centered on the pixel of interest. Fig. 5 shows a comparison of the original clustering result with the smoothed labels on a subsection of the full image. It is possible to note that many of the small (but irrelevant for the task at hand) details have been removed.

The final step of the algorithm aimed at converting the unsupervised clustering results into a usable "flood detection map" through the use of domain-knowledge of the sensor and problem. Specifically, the first step towards flood detection was to apply clustering to find pixels which were likely to be water. This cluster was identified using the fact that water is more absorptive in the NIR wavelengths. Therefore, the cluster having the lowest average NIR intensity was then considered as the one in which pixels were most likely to be water.

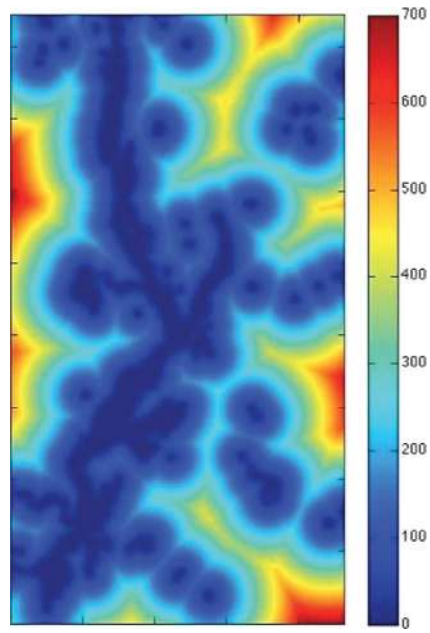

Fig. 6. Result of applying distance transform to the "water" pixels.

TABLE V
CONFUSION MATRIX AND K COEFFICIENT OR THE UNSUPERVISED CHANGE DETECTION—OPTICAL DATA

		Prediction		
	$K = 0.688$	Change	No Change	%
True	Change	682,820	181,164	**78.7**
	No Change	355,108	8,571,308	**96.3**
	%	**67.7**	**97.9**	

The low NIR spectral rule identified the majority of the water flooded regions, but it yielded many false positives that were far away from the central flooded region. To remove these false positives, only pixels close to the largest central water regions were retained. These regions were mostly connected, but required some further processing to fill-in the holes. To this end, a distance transform was applied to the image. The transform labeled each non-water pixel by its distance to the closest water sample. Then, clusters within a distance of less than 15 pixels were retained along with the original water samples. Fig. 6 shows the results of the distance transform. To remove the false positives, only the two largest connected components were retained. This rule maintained the flooded areas and disregarded the water and false positive areas far from the river.

The final submission produced a K coefficient of 0.688. The confusion matrix in Table V further details the distribution of accurately predicted change detection pixels.

VII. A Predictive Method for Projected Post-Flood Change Detection

When a disaster strikes, the first few hours are critical to coordinate the response. Important decisions have to be made regarding where to send the first available rescue teams, how the transport and communication networks have been impacted, and whether some population are threaten by disaster developments, such as new flooding, tsunami, or earthquake replicas. Unfortunately, in the first few hours of the disaster mitigation period, rescue resources are scarce. Given that lives are at stake, the importance of allocating these resources efficiently is paramount. These decisions require the clearest view of the situation, with the most up-to-date information available. Yet, local monitoring of the place where the disaster struck is often affected and, depending on the topography of the area, it may be difficult to bear new monitoring teams and devices from neighboring places.

In this situation, satellites are invaluable tools: their operation is not affected by the local crisis, they provide global coverage and are able to acquire several large areas at a time. However, satellites are not able to provide real time imagery. As an example, weather is a factor that may delay the acquisition of optical imagery. This is particularly true in the case of flooding, where cloud cover is indicative of the event. Further, many areas in the world have an average cloud coverage higher than 80%, which increases the average delay before high-quality spaceborne optical images are available. In the case of the International Charter, the delay between the disaster and the first images is at least 1 or 2 days, and sometimes even longer [52], whereas the COSMO-SkyMed constellations has 12 hour revisit time under emergency conditions. Therefore, it may be important to start evaluating the area of the event even before the first post-event image comes. At this stage, any information is useful.

Many sources are available concerning pre-disaster imagery, for most places; Google Earth or Bing Maps enable to examine places for a better idea about where the risks may be concentrated (usually in the settlements), Landsat imagery is available globally, and archived images of the area are commonly available in data provider's catalogs. For flood events, these images and map sources can be complemented with another source of information: the elevation map. Initiatives like the Shuttle Radar Topography Mission (SRTM) or the Advanced Spaceborne Thermal Emission and Reflection Radiometer (ASTER) provide a reliable elevation map for any place between latitude 60 North and latitude 60 South for SRTM and between latitude 83 North and latitude 83 South for ASTER. This provides coverage for most of the world population.

On the other hand, the data available also varies significantly in nature and quality. So it is critical to have flexible tools to deal with unexpected situations. For this study, the Orfeo Toolbox (OTB) [53] was used. OTB is an open-source image processing library which handles image geometry and map projection, access a variety of data, such as digital elevation models, and standard image processing techniques in a flexible and integrated way. This tool provides advanced algorithms as well as low level access to data.

In the case of the Contest, several facts made it easier to use the information derived from the DEM. In fact, the terrain was relatively flat, without sharp mountains, and the objective was to measure the flood extension a few hours after it happened.

Fig. 7. SRTM DEM of the flooded area.

TABLE VI
Confusion Matrix and K Coefficient for the Predictive Method

		Prediction		
	$K = 0.627$	Change	No Change	%
True	Change	583,847	280,137	**67.5**
	No Change	318,769	8,607,647	**96.4**
	%	**64.6**	**96.8**	

The metadata included in the images is critical to understand the context. However, the before-flood SPOT image had the wrong metadata providing a wrong geolocation. Unfortunately, this kind of situation is common in real-case scenarios and should be accounted for. It is important to be cautious of this information at any time and it is another reason why flexible tools are critical.

Fig. 7 shows the SRTM DEM extracted from the metadata of the post-event SPOT image. Using a flood level of 13 m above sea level, the flood detection accuracy was 0.627, which was a reasonable value compared to other results in these difficult conditions. The confusion matrix in Table VI further details the distribution of accurately predicted change detection pixels.

VIII. Discussion and Conclusion

At the end of the Contest, more than 200 users downloaded the data set and more than 350 different change detection maps have been uploaded to the system to be ranked. In general, the Contest turned out to be very tough for the methods in all the categories, as evidenced by a maximum accuracy of 0.703. The relatively low accuracy may be due to the presence of pixel level region mixing issue, in which an isolated patch of dry area surrounded by water may be considered as flood by a human operator that defines the extension of the flooded area. Further, the flooded area changed significantly between the two sensor observations (about 4 days apart). This may have created fundamentally different information, increasing the difficulty to deal with the temporal shift between the optical and SAR data sets.

The top-ranked change detection maps submitted for each category are shown in Fig. 8, whereas the relative best accuracies are reported in Table VII. As shown, the methods that

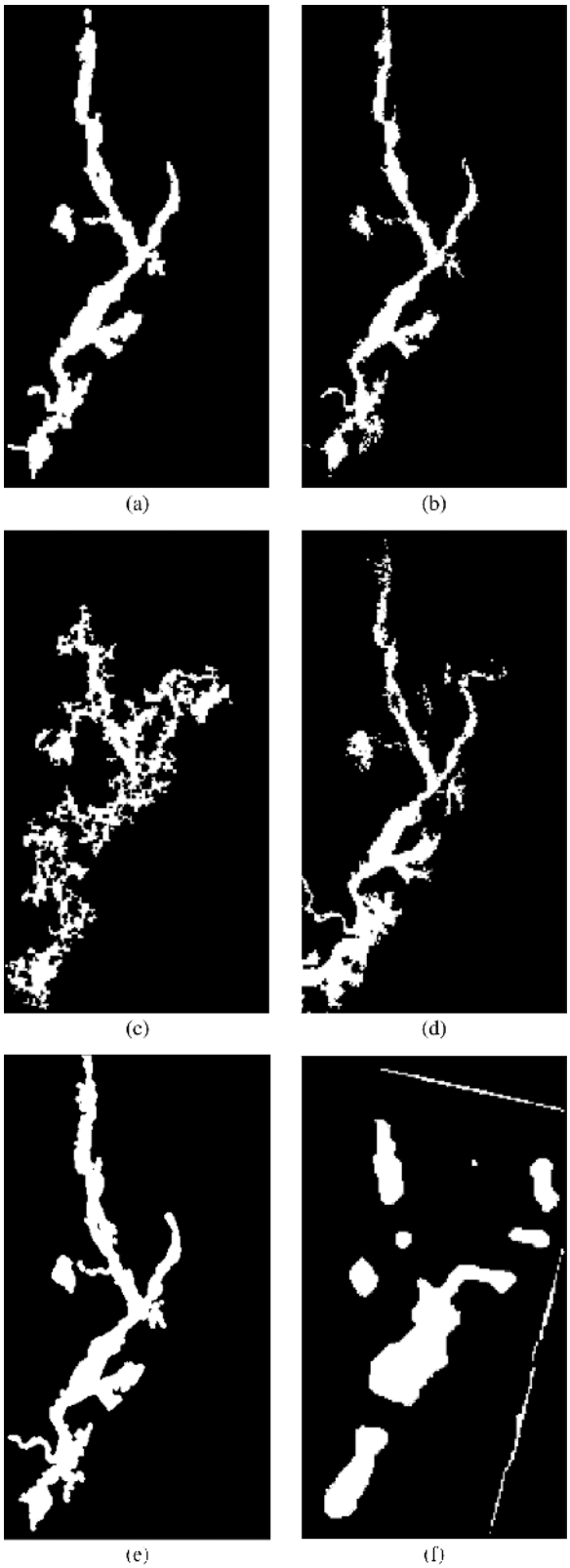

Fig. 8. Top-ranked maps that were submitted for each category: (a) Supervised—All data, (b) Supervised—Optical data, (c) Supervised—SAR data, (d) Unsupervised—All data, (e) Unsupervised—Optical data, (f) Unsupervised—SAR data.

exploited SAR imagery alone did not provide accurate change detection maps. For the "Supervised—SAR data" category, the method in [54] was exploited. For the "Unsupervised—SAR data" category a patch-based similarity between the two SAR images was computed at each pixel for different patch sizes.

TABLE VII
K COEFFICIENT OF THE BEST RESULT FOR EACH CATEGORY

Category	K coefficient
Supervised - All data	0.703
Supervised - Optical data	0.650
Supervised - SAR data	0.387
Unsupervised - All data	0.627
Unsupervised - Optical data	0.688
Unsupervised - SAR data	0.476
Majority Voting (best 5 individual results)	0.706

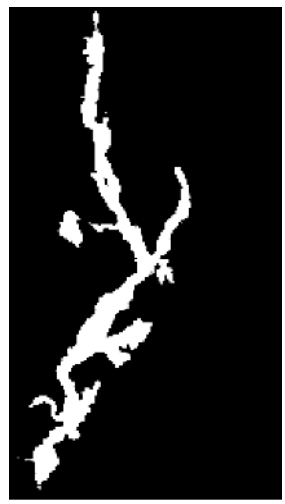

Fig. 9. Decision fusion result produced using majority voting between the best 5 individual results among all submissions.

TABLE VIII
CONFUSION MATRIX AND K COEFFICIENT FOR THE DECISION FUSION RESULT

		Prediction		
	$K = 0.706$	Change	No Change	%
True	Change	635,457	228,527	**73.5**
	No Change	236,920	8,689,496	**97.3**
	%	**72.8**	**97.4**	

The decision fusion of the best 5 individual results among all submissions was achieved using majority voting (shown in Fig. 9). Table VIII presents the corresponding final confusion matrix. The K coefficient was 0.706. Even though the final score is less than 1% higher than the best algorithm, majority voting still outperformed all the other results submitted on this data set. Further, the statistical significance of the change detection maps was evaluated with the McNemar test and all the results were statistically significant (to the 95% confidence level).

Failure or success of a change detection algorithm cannot be analyzed only with a confusion matrix, as it is important to understand the context of the application. For example, missed alarms may be more important than a false alarm in catastrophic scenarios as it is better to check a non-destroyed building than not to visit a destroyed one. For the flood detection application discussed in this paper, the number of true positives and true negatives of the confusion matrices reported in Tables III–VI

were approximately the same for all the winning methods. The main differences can be found in the off-diagonal terms. The "Supervised—Optical data" and "Unsupervised—Optical data" entries showed the opposite behavior, the first having about twice false negatives than false positives, and the second having about twice false positives compared to the false negatives. The submissions "Supervised—All data" and "Unsupervised—All data" showed more balance values along the off-diagonal terms. This was also the case of the decision fusion confusion matrix.

All the proposed methods relied on different modeling solutions and showed different ways to approach the change detection problem. However, it is important to emphasize that physical properties (such as the admissible distance from water and the elevation information extracted from the DEM) have been successfully used in addition to traditional approaches based on pattern recognition, image processing techniques, and contextual information. These approaches open new research possibilities for data fusion, where integration of the physics of the problem may play an important role for the success of the modeling task involving complex phenomena.

Further, it is important to highlight the small difference in accuracy achieved between supervised and unsupervised methods. This is remarkable considering the quick response that may be necessary in disaster scenarios without training samples available. For the case of a flood event, this study also showed that even without up-to-date data, reasonable results can be obtained within minutes of the flood crisis (and even before the flood event itself) with a DEM-based predictive model. Of course, combining this early information with post-event images may further improve the results. Additionally, the elevation map can be, for instance, used as a further input for the classification phase.

To conclude, in a relatively recent paper [55], Wilkinson showed satellite image classification results have not been improving over the past 20 years. This is corroborated by the results of this Contest, where the various machine learning techniques have shown little difference to the general classification problem. Specifically, older methods, such as the supervised neural network and the unsupervised C-mean, provided the same level of accuracy as did newer methods. As a matter of fact, the exact same neural network approach provided the best individual performance among all submissions in the previous 2007 and 2008 Contests [3], [4]. These conclusions suggest that research should be directed to investigating new and more powerful input features (as an example, multi-temporal as well as multi-angular information can be exploited) to be fed into the various machine learning schemes, or to a better understanding of the physical behavior of the Earth surface being investigated.

REFERENCES

[1] 2011, IEEE GRSS Data Fusion Technical Committee. [Online]. Available: http://www.grss-ieee.org/community/technical-committees/data-fusion/

[2] L. Alparone, L. Wald, J. Chanussot, C. Thomas, P. Gamba, and L. M. Bruce, "Comparison of pansharpening algorithms: Outcome of the 2006 GRS-S data fusion contest," *IEEE Trans. Geosci. Remote Sens.*, vol. 45, no. 10, pp. 3012–3021, Oct. 2007.

[3] F. Pacifici, F. Del Frate, W. Emery, P. Gamba, and J. Chanussot, "Urban mapping using coarse SAR and optical data: Outcome of the 2007 GRSS data fusion contest," *IEEE Geosci. Remote Sens. Lett.*, vol. 5, no. 3, pp. 331–335, Jul. 2008.

[4] G. Licciardi, F. Pacifici, D. Tuia, S. Prasad, T. West, F. Giacco, C. Thiel, J. Inglada, E. Christophe, J. Chanussot, and P. Gamba, "Decision fusion for the classification of hyperspectral data: Outcome of the 2008 GRS-S data fusion contest," *IEEE Trans. Geosci. Remote Sens.*, vol. 47, no. 11, pp. 3857–3865, Nov. 2009.

[5] P. Coppin, I. Jonckheere, K. Nackaerts, and M. B., "Digital change detection methods in ecosystem monitoring: A review," *Int. J. Remote Sens.*, vol. 25, no. 9, pp. 1565–1596, 2004.

[6] A. Singh, "Digital change detection techniques using remotely-sensed data," *Int. J. Remote Sens.*, vol. 10, no. 6, pp. 989–1003, 1989.

[7] F. D. Frate, F. Pacifici, and D. Solimini, "Monitoring urban land cover in Rome, Italy and its changes by single-polarization multi-temporal SAR images," *IEEE J. Sel. Topics Appl. Earth Observ. Remote Sens.*, vol. 1, no. 2, pp. 87–97, Jun. 2008.

[8] F. Pacifici, F. D. Frate, C. Solimini, and W. Emery, "An innovative neural-net method to detect temporal changes in high-resolution optical satellite imagery," *IEEE Trans. Geosci. Remote Sens.*, vol. 45, no. 9, pp. 2940–2952, 2007.

[9] J. Chen, X. Chen, X. Cui, and J. Chen, "Change vector analysis in posterior probability space: A new method for land cover change detection," *IEEE Geosci. Remote Sens. Lett.*, vol. PP, no. 99, pp. 317–321, 2010.

[10] W. A. Malila, "Change vector analysis: An approach for detecting forest change with Landsat," in *IEEE Proc. Annual Symp. Machine Processing of Remotely Sensing Data*, 1980, pp. 326–336.

[11] F. Bovolo and L. Bruzzone, "A split-based approach to unsupervised change detection in large size multitemporal images: Application to Tsunami-damage assessment," *IEEE Trans. Geosci. Remote Sens.*, vol. 45, no. 6, pp. 1658–1671, 2007.

[12] H. Nemmour and Y. Chibani, "Multiple support vector machines for land cover change detection: An application for mapping urban extensions," *J. Photogr. Remote Sens.*, vol. 61, pp. 125–133, 2006.

[13] G. Camps-Valls, L. Gómez-Chova, J. Muñoz-Marí, J. L. Rojo-Álvarez, and M. Martínez-Ramón, "Kernel-based framework for multi-temporal and multi-source remote sensing data classification and change detection," *IEEE Trans. Geosci. Remote Sens.*, vol. 46, no. 6, pp. 1822–1835, 2008.

[14] F. Bovolo, L. Bruzzone, and M. Marconcini, "A novel approach to unsupervised change detection based on a semisupervised SVM and a similarity measure," *IEEE Trans. Geosci. Remote Sens.*, vol. 46, no. 7, pp. 2070–2082, Jul. 2008.

[15] J. Muñoz-Marí, F. Bovolo, L. Gómez-Chova, L. Bruzzone, and G. Camps-Valls, "Semisupervised one-class support vector machines for classification of remote sensing data," *IEEE Trans. Geosci. Remote Sens.*, vol. 48, no. 8, pp. 3188–3197, 2010.

[16] T. N. Tran, R. Wehrens, and L. M. C. Buydens, "Sparef: A clustering algorithm for multispectral images," *Analytica Chimica Acta* vol. 490, no. 1–2, pp. 303–312, 2003 [Online]. Available: http://www.sciencedirect.com/science/article/pii/S0003267003007207, papers presented at the 8th International Conference on Chemometrics and Analytical Chemistry

[17] M. Hasanzadeh and S. Kasaei, "A multispectral image segmentation method using size-weighted fuzzy clustering and membership connectedness," *IEEE Geosci. Remote Sens. Lett.*, vol. 7, no. 3, pp. 520–524, Jul. 2010.

[18] A. Marcal and L. Castro, "Hierarchical clustering of multispectral images using combined spectral and spatial criteria," *IEEE Geosci. Remote Sens. Lett.*, vol. 2, no. 1, pp. 59–63, Jan. 2005.

[19] G. Hazel, "Multivariate Gaussian MRF for multispectral scene segmentation and anomaly detection," *IEEE Trans. Geosci. Remote Sens.*, vol. 38, no. 3, pp. 1199–1211, May 2000.

[20] G. Martin and A. Plaza, "Region-based spatial preprocessing for endmember extraction and spectral unmixing," *IEEE Geosci. Remote Sens. Lett.*, vol. 8, no. 4, pp. 745–749, Jul. 2011.

[21] A. Zare, O. Bchir, H. Frigui, and P. Gader, "Spatially-smooth piecewise convex endmember detection," in *2010 2nd Workshop on Hyperspectral Image and Signal Processing: Evolution in Remote Sensing (WHISPERS)*, Jun. 2010, pp. 1–4.

[22] M. Zortea and A. Plaza, "Spatial preprocessing for endmember extraction," *IEEE Trans. Geosci. Remote Sens.*, vol. 47, no. 8, pp. 2679–2693, Aug. 2009.

[23] A. Zare, J. Bolton, P. Gader, and M. Schatten, "Vegetation mapping for landmine detection using long-wave hyperspectral imagery," *IEEE Trans. Geosci. Remote Sens.*, vol. 46, no. 1, pp. 172–178, Jan. 2008.

[24] D. Chaudhuri and A. Samal, "An automatic bridge detection technique for multispectral images," *IEEE Trans. Geosci. Remote Sens.*, vol. 46, no. 9, pp. 2720–2727, Sep. 2008.
[25] Y. Bazi, L. Bruzzone, and F. M. Melgani, "An unsupervised approach based on the generalized Gaussian model to automatic change detection in multitemporal SAR images," *IEEE Trans. Geosci. Remote Sens.*, vol. 43, no. 4, pp. 874–887, April 2005.
[26] G. Moser and S. B. Serpico, "Generalized minimum-error thresholding for unsupervised change detection from SAR amplitude imagery," *IEEE Trans. Geosci. Remote Sens.*, vol. 44, no. 10, pp. 2972–2982, Oct. 2006.
[27] C. Carincotte, S. Derrode, and S. Bourennane, "Unsupervised change detection on SAR images using fuzzy hidden Markov chains," *IEEE Trans. Geosci. Remote Sens.*, vol. 44, no. 2, pp. 432–441, Feb. 2006.
[28] T. Hastie, R. Tibshirani, and J. Friedman, *The Elements Of Statistical Learning: Data Mining, Inference, and Prediction*, 2nd ed. New York: Springer, 2009.
[29] J. F. Mas and J. J. Flores, "The application of artificial neural networks to the analysis of remotely sensed data," *Int. J. Remote Sens.*, vol. 29, no. 3, pp. 617–663, Feb. 2008.
[30] J. Benediktsson, P. Swain, and O. Ersoy, "Neural network approaches versus statistical methods in classification of multisource remote sensing data," *IEEE Trans. Geosci. Remote Sens.*, vol. 28, no. 4, pp. 540–552, Jul. 1990.
[31] S. Gopal and C. Woodcock, "Remote sensing of forest change using artificial neural networks," *IEEE Trans. Geosci. Remote Sens.*, vol. 34, no. 2, pp. 398–404, Mar. 1996.
[32] G. Carpenter, S. Gopal, B. Shock, and C. Woodcock, A neural network method for land use change classification, with application to the Nile river delta Boston Univ., Ctr. Adaptive Systems, Dept. Cognitive and Neural Systems, Boston, MA, Tech. Rep., 2001 [Online]. Available: http://techlab.bu.edu/files/resources/articles_cns/CarpenterGopal-ShockWoodcock2003.pdf
[33] I. Olthof, "Mapping deciduous forest ice storm damage using Landsat and environmental data," *Remote Sens. Environ.*, vol. 89, no. 4, pp. 484–496, Feb. 2004.
[34] S. Ghosh, L. Bruzzone, S. Patra, F. Bovolo, and A. Ghosh, "A context-sensitive technique for unsupervised change detection based on hopfield-type neural networks," *IEEE Trans. Geosci. Remote Sens.*, vol. 45, no. 3, pp. 778–789, Mar. 2007.
[35] F. Pacifici and W. J. Emery, *Pulse Coupled Neural Networks for Automatic Urban Change Detection at Very High Spatial Resolution*, ser. Lecture Notes in Computer Science. Berlin, Heidelberg, Germany: Springer, 2009, vol. 5856, pp. 929–942.
[36] M. Chini, F. Pacifici, W. Emery, N. Pierdicca, and F. Del Frate, "Comparing statistical and neural network methods applied to very high resolution satellite images showing changes in man-made structures at rocky flats," *IEEE Trans. Geosci. Remote Sens.*, vol. 46, no. 6, pp. 1812–1821, Jun. 2008.
[37] J. Sola and J. Sevilla, "Importance of input data normalization for the application of neural networks to complex industrial problems," *IEEE Trans. Nucl. Sci.*, vol. 44, no. 3, pp. 1464–1468, Jun. 1997.
[38] F. Pacifici, M. Chini, and W. J. Emery, "A neural network approach using multi-scale textural metrics from very high resolution panchromatic imagery for urban land-use classification," *Remote Sens. Environ.*, vol. 113, no. 6, pp. 1276–1292, Jun. 2009.
[39] J. Serra, *Image Analysis and Mathematical Morphology*. New York: Academic Press, 1982.
[40] P. Soille, *Morphological Image Analysis*, 2nd ed. Berlin, Germany: Springer, 2004.
[41] M. Fauvel, J. A. Benediktsson, J. Chanussot, and J. R. Sveinsson, "Spectral and spatial classification of hyperspectral data using SVMs and morphological profiles," *IEEE Trans. Geosci. Remote Sens.*, vol. 46, no. 11, pp. 3804–3814, 2008.
[42] D. Tuia, F. Pacifici, M. Kanevski, and W. Emery, "Classification of very high spatial resolution imagery using mathematical morphology and support vector machines," *IEEE Trans. Geosci. Remote Sens.*, vol. 47, no. 11, pp. 3866–3879, 2009.
[43] D. Tuia, G. Camps-Valls, G. Matasci, and M. Kanevski, "Learning relevant image features with multiple kernel classification," *IEEE Trans. Geosci. Remote Sens.*, vol. 48, no. 10, pp. 3780–3791, 2010.
[44] M. Dalla Mura, J. A. Benediktsson, F. Bovolo, and L. Bruzzone, "An unsupervised technique based on morphological filters for change detection in very high resolution images," *IEEE Trans. Geosci. Remote Sens.*, vol. 5, no. 3, pp. 433–437, 2008.
[45] F. Bovolo, "A multilevel parcel-based approach to change detection in very high resolution multitemporal images," *IEEE Geosci. Remote Sens. Lett.*, vol. 6, no. 1, pp. 33–38, 2009.
[46] M. Volpi, D. Tuia, F. Bovolo, M. Kanevski, and L. Bruzzone, "Supervised change detection in VHR images using contextual information and support vector machines," *Int. J. Appl. Earth Observ. Geoinform.*, 2011, in press.
[47] M. Pesaresi and J. Benediktsson, "A new approach for the morphological segmentation of high-resolution satellite images," *IEEE Trans. Geosci. Remote Sens.*, vol. 39, no. 2, pp. 309–320, 2001.
[48] J. A. Benediktsson, M. Pesaresi, and K. Arnason, "Classification and feature extraction for remote sensing images from urban areas based on morphological transformations," *IEEE Trans. Geosci. Remote Sens.*, vol. 41, no. 9, pp. 1940–1949, 2003.
[49] R. Collobert, S. Bengio, and J. Mariéthoz, "Torch: A Modular Machine Learning Software Library," IDIAP, Tech. Rep. RR 02-46, 2002.
[50] T. N. Tran, R. Wehrens, and L. M. Buydens, "Clustering multispectral images: A tutorial," *Chemometrics and Intelligent Laboratory Systems*, vol. 77, no. 1–2, pp. 3–17, 2005.
[51] C. Yang, L. Bruzzone, F. Sun, L. Lu, R. Guan, and Y. Liang, "A fuzzy-statistics-based affinity propagation technique for clustering in multispectral images," *IEEE Trans. Geosci. Remote Sens.*, vol. 48, no. 6, pp. 2647–2659, Jun. 2010.
[52] Disaster charter. [Online]. Available: http://www.disasterscharter.org/home
[53] The Orfeo Team. [Online]. Available: http://www.orfeo-toolbox.org
[54] G. Mercier, G. Moser, and S. Serpico, "Conditional copula for change detection on heterogeneous SAR data," *IEEE Trans. Geosci. Remote Sens.*, vol. 45, no. 5, pp. 1428–1441, May 2008.
[55] G. Wilkinson, "Results and implications of a study of fifteen years of satellite image classification experiments," *IEEE Trans. Geosci. Remote Sens.*, vol. 43, no. 3, pp. 433–440, Mar. 2005.

Nathan Longbotham (S'11) is currently a Ph.D. student studying remote sensing in the Department of Aerospace Engineering Sciences at the University of Colorado at Boulder. He received an M.S. degree in optical science and engineering from the University of New Mexico and a B.S. degree in physics (*magna cum laude*; university scholar; presidential scholar) from Abilene Christian University.

While pursuing the M.S. degree, he held a graduate internship position at Sandia National Laboratories, where he conducted research into the properties of Q-switched microlasers and their applicability to LIDAR systems. Prior to his current studies, he held an Optical Engineer position with the holographic data storage startup, InPhase Technologies, developing a specialized, tunable ultraviolet laser system. He is currently a Research Assistant at the University of Colorado at Boulder collaborating with the R&D department at DigitalGlobe in Longmont, CO, developing urban remote sensing techniques that leverage multi-angle optical imagery. His research interests include image analysis, data fusion, multi-temporal data analysis, and feature extraction.

Mr. Longbotham earned first place in the 2009 IEEE Geoscience and Remote Sensing Data Fusion Contest. He serves as a reviewer for the IEEE JOURNAL OF SELECTED TOPICS IN APPLIED EARTH OBSERVATION AND REMOTE SENSING.

Fabio Pacifici (S'03–M'10) received the Ph.D. degree in GeoInformation from Tor Vergata University, Rome, Italy, in 2010. He also received the Laurea Specialistica (M.S.; *cum laude*) and Laurea (B.S.; *cum laude*) degrees in telecommunication engineering from the same University, in 2003 and 2006, respectively.

Since 2009, he is working at DigitalGlobe as R&D Scientist. Between 2005 and 2009, he collaborated as Visitor Scientist with the Department of Aerospace Engineering Sciences, University of Colorado, Boulder. He has been involved in various remote sensing projects supported by the European Space Agency. His research activities include processing of remote sensing images, data fusion, feature extraction, active learning, and analysis of multitemporal data. In particular, his research interests are related to the development of classification and change detection techniques for urban remote sensing applications using very high spatial resolution optical and/or synthetic aperture radar imagery, with special emphasis on machine learning. He is author (or co-author) of 13 scientific publications in referred international Journals, 2 book chapters, and more than 40 contributions in international conferences.

Dr. Pacifici is the current Chair of the IEEE Geoscience and Remote Sensing Data Fusion Technical Committee and serves as Associate Editor for the IEEE JOURNAL OF SELECTED TOPICS IN APPLIED EARTH OBSERVATIONS AND REMOTE SENSING (JSTARS). He was the recipient of the 2009 Joint Urban Remote Sensing Event student paper competition. He received the first prize in the 2007, 2008 and the 2009 IEEE Geoscience and Remote Sensing Data Fusion Contest. He served as a member of the 2011 Joint Urban Event Technical Committee and Session Chair at the International Geoscience and Remote Sensing Symposium. He has been the Guest Editor of a special issue of the JSTARS on multiangular remote sensing.

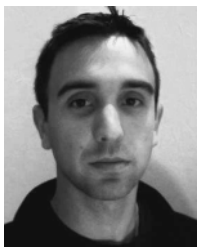

Taylor Glenn (S'10) received the B.S. and M.E. degrees in computer engineering from the University of Florida, Gainesville, in 2003 and 2004. He is currently a Ph.D. candidate and Graduate Fellow in the Department of Computer and Information Science and Engineering at the University of Florida.

From 2004 to 2009 he was a partner and lead engineer at 2G Engineering, LLC. His current research interests are in the fields of machine learning, computer vision, and remote sensing.

Alina Zare (M'08) received the Ph.D. degree in computer engineering from the University of Florida in December 2008.

She is an Assistant Professor in the Department of Electrical and Computer Engineering at the University of Missouri, Columbia. Her research interests include remote sensing, sparsity promotion, machine learning, image analysis, and pattern recognition. She has been involved in landmine, explosive object and trace explosives detection research using hyperspectral imagers in a variety of modalities such airborne or ground-based forward-looking sensors. She has also conducted research on target detection using wideband electromagnetic induction sensors and investigated agent-based modeling techniques for human geography applications.

Michele Volpi (S'08) was born in Lugano, Switzerland, in 1985. He received the B.S. degree in physical geography and the M.S. degree in environmental sciences from the University of Lausanne, Lausanne, Switzerland, in 2007 and in 2009, respectively. He is currently pursuing the Ph.D. degree at the Institute of Geomatics and Analysis of Risk, University of Lausanne, under a Swiss National Science Foundation grant.

His research activities are in the area of remote sensing image processing and multitemporal image analysis. In particular, his interests include the development and application of machine learning algorithms (specifically kernel-based methods) for change detection, multitemporal image classification, feature extraction, and classification for multispectral very high resolution data.

Mr. Volpi was one of the winners of the IEEE Geosciences and Remote Sensing Data Fusion Contest, in 2009. He is a referee of IEEE TRANSACTIONS ON GEOSCIENCE AND REMOTE SENSING and *IEEE Geoscience and Remote Sensing Letters*.

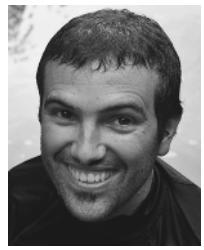

Devis Tuia (S'07–M'09) was born in Mendrisio, Switzerland, in 1980. He received the diploma in Geography at the University of Lausanne in 2004, the Master of Advanced Studies in Environmental Engineering at the Federal Institute of Technology of Lausanne (EPFL) in 2005, and the Ph.D. in environmental sciences at the University of Lausanne in 2009.

He was a postdoc researcher at both the University of Valéncia, Spain and the Univeristy of Colorado at Boulder under a Swiss National Foundation program. He is now a Senior Research Associate at the Laboratoire des Systèmes d'Information Géographiques, EPFL. His research interests include the development of algorithms for information extraction and classification of very high resolution remote sensing images and socio-economic data using machine learning algorithms. His website is http://devis.tuia.googlepages.com/.

Emmanuel Christophe (M'07) received the Engineering degree in Telecommunications from École Nationale Supérieure des Télécommunications de Bretagne, Brest, France, and the DEA in Telecommunications and image processing from University of Rennes 1 in 2003. In October 2006, he received the Ph.D. degree from Supaero and University of Toulouse in hyperspectral image compression and image quality.

He has been a visiting scholar in 2006 at Rensselaer Polytechnic Institute, Troy, NY, USA. From 2006 to 2008, he was a research engineer at CNES, the French Space Agency, focusing on information extraction for high resolution optical images. Between 2008 and 2010, he moved to Singapore at CRISP, National University of Singapore, where he was tackling new challenges for remote sensing in tropical areas. He is now with Google Inc. in California.

Julien Michel (A'10) received the Telecommunications Engineer degree from the École Nationale Supérieure des Télécommunications de Bretagne, Brest, France, in 2006.

From 2006 to 2010, he has been with Communications et Systèmes, Toulouse, France, where he has been working on studies and developments in the field of remote sensing image processing. He is now with the Centre National d'Études Spatiales (French Space Agency), Toulouse, France, where he is in charge of the development of image processing algorithms for the exploitation of Earth observation images, mainly in the field of very high resolution image analysis.

Jordi Inglada (M'09) received the Telecommunications Engineer degree from both the Universitat Politècnica de Catalunya, Barcelona, Spain, and the École Nationale Supérieure des Télécommunications de Bretagne, Brest, France, in 1997 and the Ph.D. degree in signal processing and telecommunications in 2000 from Université de Rennes 1, Rennes, France.

He is currently with the Centre National d'Études Spatiales (French Space Agency), Toulouse, France, working in the field of remote sensing image processing at the CESBIO laboratory. He is in charge of the development of image processing algorithms for the operational exploitation of Earth observation images, mainly in the field of multitemporal image analysis for land use and cover change.

Dr. Inglada is an Associate Editor of the IEEE TRANSACTIONS ON GEOSCIENCE AND REMOTE SENSING.

Jocelyn Chanussot (M'04–SM'04–F'12) received the M.Sc. degree in electrical engineering from the Grenoble Institute of Technology (Grenoble INP), Grenoble, France, in 1995, and the Ph.D. degree from Savoie University, Annecy, France, in 1998.

In 1999, he was with the Geography Imagery Perception Laboratory for the Delegation Generale de l'Armement (DGA—French National Defense Department). Since 1999, he has been with Grenoble INP, where he was an Assistant Professor from 1999 to 2005, an Associate Professor from 2005 to 2007, and is currently a Professor of signal and image processing. He is currently conducting his research at the Grenoble Images Speech Signals and Automatics Laboratory (GIPSA-Lab). His research interests include image analysis, multicomponent image processing, nonlinear filtering, and data fusion in remote sensing.

Dr. Chanussot is the founding President of IEEE Geoscience and Remote Sensing French chapter (2007–2010) which received the 2010 IEEE GRS-S Chapter Excellence Award "for excellence as a Geoscience and Remote Sensing Society chapter demonstrated by exemplary activities during 2009." He was the recipient of the 2011 IEEE GRSS Symposium Best Paper Award. He was a member of the IEEE Geoscience and Remote Sensing Society AdCom (2009–2010), in charge of membership development. He was the General Chair of the first IEEE GRSS Workshop on Hyperspectral Image and Signal Processing, Evolution in Remote sensing (WHISPERS). He was the Chair (2009–2011) and the Co-Chair (2005–2008) of the GRS Data Fusion Technical Committee. He was a member of the Machine Learning for Signal Processing Technical Committee of the IEEE Signal Processing Society (2006–2008) and the Program Chair of the IEEE International Workshop on Machine Learning for Signal Processing, (2009). He was an Associate Editor for the IEEE Geoscience And Remote Sensing Letters (2005–2007) and for Pattern Recognition (2006–2008). Since 2007, he has been an Associate Editor for the IEEE TRANSACTIONS ON GEOSCIENCE AND REMOTE SENSING. Since 2011, he has been the Editor-in-Chief of the IEEE JOURNAL OF SELECTED TOPICS IN APPLIED EARTH OBSERVATIONS AND REMOTE SENSING.

Qian Du (S'98–M'00–SM'05) received the Ph.D. degree in electrical engineering from the University of Maryland Baltimore County in 2000.

She was with the Department of Electrical Engineering and Computer Science, Texas A&M University, Kingsville, from 2000 to 2004. She joined the Department of Electrical and Computer Engineering at Mississippi State University in Fall 2004, where she is currently an Associate Professor. Her research interests include hyperspectral remote sensing image analysis, pattern classification, data compression, and neural networks.

Dr. Du currently serves as Co-Chair for the Data Fusion Technical Committee of IEEE Geoscience and Remote Sensing Society. She also serves as Associate Editor for IEEE JOURNAL OF SELECTED TOPICS IN APPLIED EARTH OBSERVATIONS AND REMOTE SENSING (J-STARS). She received the 2010 Best Reviewer award from IEEE Geoscience and Remote Sensing Society. She is the General Chair for the fourth IEEE GRSS Workshop on Hyperspectral Image and Signal Processing, Evolution in Remote Sensing (WHISPERS). Dr. Du is a member of SPIE, ASPRS, and ASEE.